STUDY OF PASSIVELY STABLE, FULLY DETACHED DIVERTOR PLASMA REGIMES ATTAINED IN INNOVATIVE LONG-LEGGED DIVERTOR CONFIGURATIONS

M.V. UMANSKY, M.E. RENSINK
Lawrence Livermore National Laboratory
Livermore, CA 94550, USA
Email: umansky1@llnl.gov

B. LABOMBARD, D. BRUNNER, T. GOLFINOPOULOS, A.Q. KUANG, J.L. TERRY, D.G. WHYTE
MIT Plasma Science and Fusion Center
Cambridge, MA 02139, USA

M. WIGRAM
York Plasma Institute, University of York
York, United Kingdom

Abstract

Numerical modeling of divertor configurations with radially or vertically extended, tightly baffled, outer divertor legs demonstrates the existence of a passively stable fully detached divertor regime. In the simulations, long-legged divertors provide up to an order of magnitude increase in peak power handling capability compared to conventional divertors. The key physics for attaining the passively stable, fully detached regime in these simulations involves the interplay of strong convective plasma transport to the divertor leg outer sidewall, confinement of neutral gas in the divertor volume, geometric effects including a secondary X-point, and atomic radiation. In this regime, the detachment front location is set by the balance between the power entering the divertor leg and the losses to the walls of the divertor channel. Correspondingly, the maximum power that can be accommodated by the divertor, while still staying detached, increases with the leg length. The detached regime access window in terms of input power, core plasma density, and impurity-seeding concentration varies quantitatively depending on divertor geometry and modeling assumptions - most specifically, cross-field transport to the side walls.

1. INTRODUCTION

Due to extremely high-power exhaust densities expected for next-generation tokamaks, traditional divertor designs are likely to be inadequate for a tokamak-based fusion reactor, which prompts the search for innovative divertor designs. Some novel designs proposed in the recent years include divertors with radially extended divertor legs as in the super-X divertor [1]; the use of higher-order magnetic nulls as in the snowflake [2] and cloverleaf configurations [3]; using secondary X-points in the divertor volume or close to the target plate such as in the cusp divertor [4], X-divertor [5], and also in the inexact snowflake, i.e., snowflake-plus and snowflake-minus, configurations [2]. Exploring innovative divertor configurations by numerical modeling with edge-plasma transport codes is a valuable strategy for assessing their potential performance, before committing to experimental validation. Recently, in a computational study of divertor configurations with radially or vertically extended, tightly baffled, outer divertor legs, passively-stable fully detached divertor regimes have been found [6]. Going beyond the results described previously in Ref. [6], the present report includes a description of sensitivity studies of the model, furthermore it presents a new analysis of energetics, shedding some light on the physical mechanisms of the detached divertor regime. In particular, it explains what defines the maximum power accommodated by the divertor, what sets the location of the detachment front, and why the detachment front location is stable in this regime.

2. SIMULATION SETUP

The modeling tool used here is the edge transport code UEDGE [7] which solves plasma fluid equations in divertor geometry. We consider a configuration proposed by MIT in their conceptual design called ADX [8]. ADX is just a conceptual design at this point but ADX design parameters are available [8], and we use those parameters for this study to make a concrete example. For the dimensions and parameters of ADX, we consider target plates at different places to produce a standard vertical-plate divertor (SVPD), a super-X divertor (SXD), and an X-point-Target divertor (XPTD) [8]. In addition, we consider a long-vertical-leg divertor (LVLD) to investigate effects of radial extension of a divertor leg. We assume up-down symmetry and model only the lower half of the domain. Thus, we obtain four divertor configurations, see Fig. (1), for otherwise the same main plasma parameters and dimensions, the same physics model, same boundary conditions etc. In the model, we match the magnetic geometry, based on underlying MHD equilibrium, and set the plasma density at the separatrix according to the ADX design, 0.5×10^{20} m^{-3}. For most of the code runs we use fully recycling wall boundary conditions, and 100% neutral-particle albedo on all material surfaces; except for a few selected runs, as discussed further. To reproduce the projected ADX SOL plasma density profile width, 5 mm, we must use a radially growing diffusion coefficient $D_{\perp}$, similar to that in, e.g., Ref. [9]. On the other hand, a spatially constant $\chi_{\perp,e,i}$ is sufficient to achieve a physically looking radial profile of $T_{e,i}$ with a 3 mm width at the outer mid-plane. The power into the lower half-domain $P_{1/2}$ is used as a scan parameter and it is varied within a range relevant to ADX.

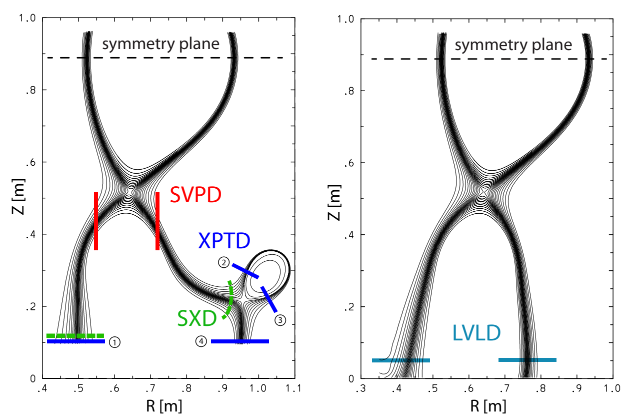

Figure 1: *Four divertor configurations based on ADX tokamak design parameters.*

The cross-field transport that provides strong interaction with the outer wall of the tokamak is a critical component of our model, ant it is based on experimental and theoretical results that go back some twenty years, showing radially outward plasma density flux extending into the far SOL [9-11]. This radially outward plasma transport is intrinsically connected with the ballistic dynamics of filamentary plasma structures in the edge [12], for which there is overwhelming evidence from tokamaks and other devices [13].

3. SIMULATION RESULTS

For the simulation results that have been described in detail in Ref. [6], here we just provide a summary for completeness. For the three long-legged divertors there is qualitatively similar behavior. For high input power the divertor is attached, and as the input power $P_{1/2}$ is lowered, keeping all other parameters fixed, the simulated divertor enters the detached state as is apparent from low plasma temperature and density near the target plates, and from high neutral gas density there. Right at the transition threshold the detachment front is localized in the divertor leg near the end, close to the target plates. As $P_{1/2}$ is lowered further, the radiation front location shifts upstream, closer to the main X-point. Eventually, as the input power $P_{1/2}$ is reduced even lower, the radiation front location shifts all way to the main X-point. As this is strongly reminiscent of the MARFE phenomenon, in these simulations this is taken as the onset of a MARFE, which sets the lower bound on the allowable input power for detached operation. In all three long-legged divertor configurations there is quite a large window in $P_{1/2}$ when the plasma is fully detached while the detachment front is still a safe distance away from the main X-point. For the standard divertor, SVPD, detached plasma might exist, but only at low input power, and the radiation front would be close to the main X-point; so, by our definition there is little, if any, range of $P_{1/2}$ for detached operation. A large parameter window with a detached divertor exists for all three long-legged configurations, while for the standard divertor (SVPD) detached plasma might exist only for very low input power. Radially or vertically extended outer legs appear beneficial for detached operation, and a long vertical leg (LVLD) permits entering detachment at about the same power as a radially extended leg (SXD). Furthermore, the secondary X-point in the outer leg (XPTD) significantly extends the detached operation window.

4. ANALYSIS AND DISCUSSION

To rule out a possibility that some numerical artifacts dominate these numerical solutions, a range of sensitivity studies have been carried out, varying parameters and assumptions in the model. Increasing the carbon impurity fraction from 1% to 2% leads to an increase of the detachment power threshold P_{det} by 10-20%. Using 1% Ne impurity instead of 1% C leads to P_{det} decreases by ~50%. Next, setting uniform transport coefficients in the outer leg only leads to P_{det} decreases by ~50%, compared to the original case where the anomalous transport coefficients are taken radially growing everywhere in the SOL. Changing the boundary conditions at the outer wall from Dirichlet to "extrapolation" (zero radial curvature) at the outer wall still leads to similar fully detached divertor solutions. Thus, varying a range of assumptions in the model leads to some quantitative changes in the results but the overall picture appears to hold.

A key observation for understanding the mechanism of stability of the detachment front was discovering a linear scaling between the maximum dissipated divertor power and the divertor leg length L_{leg}. For that, a series of UEDGE runs was carried out in the SXD configuration, varying the leg length by placing the target plate at different locations, and it was found that the maximum dissipated power at which the divertor is still detached scales linearly with the leg length, Fig. (2).

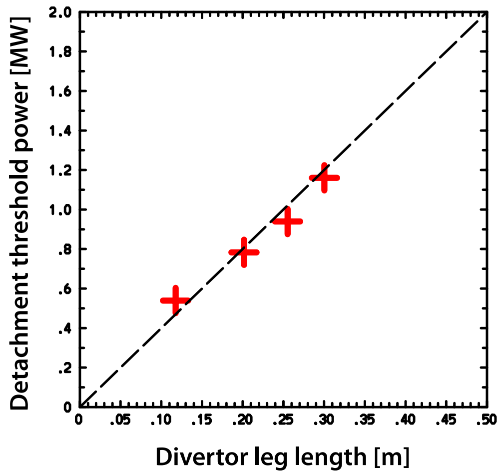

Figure 2: *The maximum dissipated power scales linearly with the length of divertor leg.*

To analyze this, for a representative detached case in an SXD configuration we looked in detail at the poloidal distribution of power flux to the outer wall, Fig. (3).

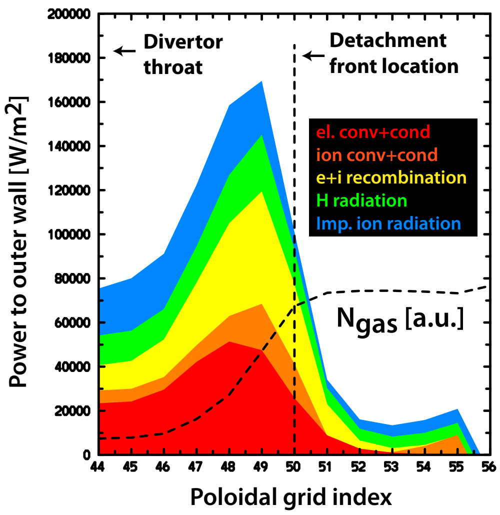

Figure 3: *Distribution of radial power flux to the wall vs. the poloidal index along the divertor leg. The radial power flux to the sidewall of the divertor channel becomes small beyond the detachment front location.*

It is found that the power flux to the outer wall of the divertor channel is small beyond the detachment front. Thus, for power dissipation the available surface area is the part of the divertor sidewall between the throat and the detachment front location. This observation explains what sets the location of the detachment front and why it is stable. Basically, the position of the detachment front is dictated by energetics; if the detachment front shifts upstream then the losses to the sidewall are reduced and there is excessive power that ionizes more neutral gas; if the detachment front shifts downstream then the energy loss to the sidewall increases, and neutral gas ionization is reduced; either way, this provides a negative feedback and restores the detachment front position.

One should note that confinement of neutral gas in the divertor volume has a strong effect on the detachment front, for cases where there is a loss of density in the divertor (using the neutral particles albedo or the plasma recycling coefficient below unity) the detachment can be lost, as discussed in detail in Ref. [6].

The divertor leg is at its limit of power dissipation (while still detached) when the detachment front is shifted all way toward the target plate; this maximizes the surface area. This is illustrated in Fig. (4), where longer and shorter divertor legs are compared side by side, for the same input power and other parameters. The spatial distribution of plasma and neutral gas parameters is the same above the detachment front. The longer leg has extra room below the detachment front, and thus it can accommodate more input power. The shorter leg is already near its limit; a small increase of input power would lead to loss of detachment and a large increase of power flux to the target plate.

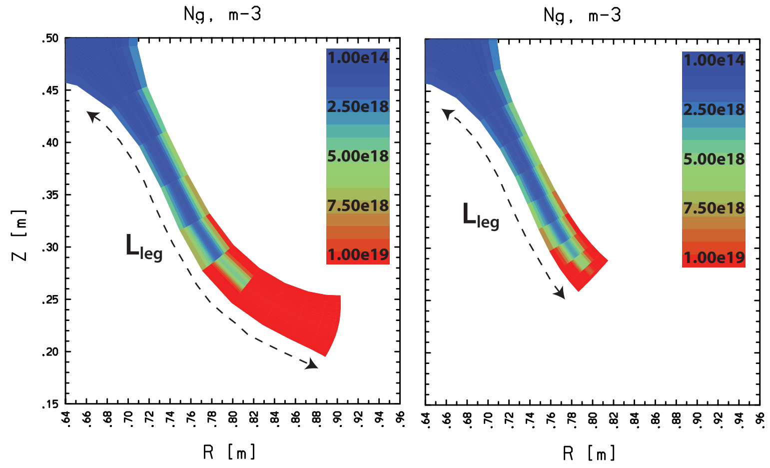

Figure 4: *For a representative case in the SXD configuration, with the same power and other parameters, distribution of neutral gas density is shown for longer and shorter divertor legs. The longer leg can accommodate more power while still staying detached while the shorter leg is already at the limit of power it can safely dissipate.*

The fully detached plasma regime in a long-legged divertor can potentially form the basis of a viable and robust solution for divertor power handling and control in a reactor and is currently considered for high-field designs (ADX, ARC). For traditional divertor solutions, the problem of detached divertor control, particularly in a neutron environment, is an unresolved challenge; and for next generation machines (ITER, ARIES, DEMO, etc.) no viable fast feedback control system has been identified. On the other hand, for a long-legged divertor, detection of the detachment front location with neutron-tolerant diagnostics can be used to monitor and control divertor plasma conditions [14].

5. CONCLUSIONS

Several tightly baffled long-legged divertor configurations have been studied with UEDGE for the parameters of ADX tokamak design, and stable steady-state fully detached regime has been found for long-legged divertors. In the simulations, in this regime the detachment power threshold is found to be up to an order of magnitude higher than for a standard divertor, and neither the plasma-facing components nor the core plasma are compromised, as the detachment front can be maintained a safe distance from the main X-point and from the target plate. The key physics for this detached divertor regime combines strong convective plasma transport to the outer wall, good confinement of neutral gas in the divertor volume, atomic radiation, and geometric effects including a secondary X-point near the target plates. In this divertor regime, energetics of plasma-material interactions in a long divertor leg provide stability of the detachment front. With several essential model assumptions varied, the overall picture of a stable fully-detached regime in tightly baffled long-legged divertor still holds, lending confidence in the overall physical picture. All in all, these simulation results suggest that a long-legged divertor holds promise for stable high-power fully-detached operation.

ACKNOWLEDGEMENTS

This material is based upon work supported by the U.S. DoE, Office of Science, Office of Fusion Energy Sciences and performed by LLNL under Contract DE-AC52-07NA27344.

REFERENCES

[1] VALANJU, P. et al., Super-X divertors and high-power density fusion devices, Phys. Plas. **70** (2009) 056110.

[2] RYUTOV, D.D., Geometrical properties of a snowflake divertor, Physics of Plasmas **14** (2007) 064502.

[3] RYUTOV, D.D. and UMANSKY, M.V Divertor with a third-order null of the poloidal field, Phys. Plas. 20 (2013) 092509.

[4] TAKASE, H. Guidance of divertor channel by cusp-like magnetic field for tokamak devices, J. Phys. Soc. Japan **70** (2001) 609.

[5] KOTSCHENREUTHER, M. Scrape off layer physics for burning plasmas and innovative divertor solutions, in: Proc. 20nd IAEA Fusion Energy Conference, IAEA, Vilamoura, Portugal, 2004, CD-ROM file IC/P6-43.

[6] UMANSKY, M.V. et al., Attainment of a stable, fully detached plasma state in innovative divertor configurations, Phys. Plasmas **24** (2017) 056112.

[7] ROGNLIEN, T.D., MILOVICH, J.L., RENSINK, M.E., PORTER, G.D., A fully implicit, time dependent 2-D fluid code for modeling tokamak edge plasmas, J. Nucl. Mater. **196–198** (1992) 347.

[8] LABOMBARD, B. et al., ADX: A high field, high power density, advanced divertor and RF tokamak, Nucl. Fusion **55** (2015) 053020.

[9] UMANSKY, M.V. et al., Modeling of particle and energy transport in the edge plasma of Alcator C-Mod, Physics of Plasmas, Volume **6,** Issue 7, pp. 2791-2796 (1999)

[10] UMANSKY, M.V. et al., Comments on particle and energy balance in the edge plasma of Alcator C-Mod Phys. Plasmas **5,** 3373 (1998)

[11] LABOMBARD, B. et al., Particle transport in the scrape-off layer and its relationship to discharge density limit in Alcator C-Mod, Nucl. Fusion **40,** 2041 (2000).

[12] KRASHENINNIKOV, S.I. On scrape off layer plasma transport Phys. Lett. A **283**, 368 (2001).

[13] DIPPOLITO, D.A. and MYRA, J.R. Cross-field blob transport in tokamak scrape-off-layer plasmas Phys. Plasmas **9**, 222 (2001).

[14] BRUNNER, D. et al., Surface heat flux feedback controlled impurity seeding experiments with Alcator C-Mods high-Z vertical target plate divertor: performance, limitations and implications for fusion power reactors Nuclear Fusion, **57**(8), (2017).